Highlights

Optimization and sizing of a fuel cell range extender vehicle for passenger car applications in driving cycle conditions

S. Molina, R. Novella, B. Pla, M. Lopez-Juarez

- Passenger FCREx components sizing and evaluation was performed for the first time
- As a novelty, the optimization comprises both the EMS and the FC system operation
- Space designs for plug-in FCV (FCREx) were generated
- Equivalent-in-range FCREx designs were compared to commercial FCV
- FCREx architecture potentially increases FCV range and efficiency (16.8%-25%)

Optimization and sizing of a fuel cell range extender vehicle for passenger car applications in driving cycle conditions

S. Molina, R. Novella*, B. Pla, M. Lopez-Juarez

CMT-Motores Térmicos, Universitat Politècnica de València
Camino de vera s/n, 46022 Valencia (Spain)

Abstract

Aiming to reduce global warming and emissions in general, cleaner technologies are the spotlight of research and industry development. Among them, fuel cell vehicles (FCV) are gaining interest to decarbonize the transport sector. Plug-in FCV or FCV in range-extender configuration (FCREx) is an interesting option to reduce the total cost of ownership (TCO) and the energy usage per km. The aim of this study was to generate design spaces of FCREx by varying the FC stack maximum power output, the battery capacity, and the H_2 tank capacity to understand the implications of this architecture in range, consumption, and cost (estimated with a WLTP driving cycle). Unlike other studies, the approach was focused on a novel architecture for passenger vehicles and was focused on the development of the validated FC system model and the energy management strategy (EMS) optimization for each design, based on the Pontryaging Minimum Principle (PMP). Consumption was found to decrease with increasing battery capacity and FC maximum power due to the higher efficiency of the systems. The design spaces showed how with 5 kg of H_2 and ≥50 kWh of battery capacity the maximum range of FCREx could be over 700 km. The results of this study showed how FCREx architecture could provide overall energy consumption saving up to 6.8% and H_2 consumption saving ranging from 16.8% to 25%, compared to current commercial FCVs. The optimum FCREx design, not only based on performance, should have ∼30 kWh of battery capacity and ≥80 kW of FC maximum power to minimize manufacturing costs while maximizing efficiency.

Keywords: Fuel cell vehicle, plug-in, Range-extender, Driving cycle, Sizing, Optimization

1. Introduction

With the growing interest in low environmental impact technologies for mobility, hydrogen fuel cell vehicles (FCVs) are getting relevant and have gained market share in the automotive industry [1]. This technology is not only relevant because it is relatively carbon-free, but also since the fuel (H_2) has many advantages as an energy carrier (section 2.1), relative to electricity for battery electric vehicles (BEVs).

As in any relatively new technology application, there exist several system architecture variations of the same technology that may improve or worsen the capabilities and performance of FCVs. This is the case of plug-in FCVs or FCVs in range-extender configuration (FCREx). FCREx configuration is a combination of BEVs and FCVs and has not yet been extensively explored for light passenger vehicles but has high potential to improve energy usage and may be the solution to extend the range of FCVs until enough H_2 refueling stations are built [2]. At present, the only architecture that was considered for light-duty passenger vehicles is that combining an FC system with a low-capacity battery. As such, the performance of FCREx architecture for passenger vehicles and how it changes with systems sizing remains unexplored, thus neglecting the potential of an FCV architecture that may be key in the context of low availability of hydrogen refueling stations.

The sizing of FCREx is relatively more complex than that of a conventional FCV since the battery capacity also affects significantly the optimum energy management strategy of the vehicle systems, the cost, and the range. As such, for this type of vehicles, it is imperative to provide a detailed and wide analysis on the performance, range, and cost of systems for different combi-

*Corresponding author:
Email address: rinoro@mot.upv.es (R. Novella)
URL: www.cmt.upv.es (R. Novella)

nations of FC system, battery capacity, and H_2 tank storage in order to understand the real potential and limits of such configuration, relative to simple FCVs.

In the literature, most of the studies focus on sizing non-plug-in FCV components [3], and those focused on FCREx [4] are not oriented towards light passenger vehicles or do not consider the same parameters as those in this study. Therefore, there is a clear lack of data regarding the sizing of FCREx systems for light-duty passenger cars.

The state-of-the-art research about FCREx for passenger vehicles is limited. As a consequence, it is difficult to assess the state-of-the-art focusing only on light-duty applications. Mainly, the recent related research lines have been focused on the use of FCREx on bus and heavy-duty applications and on the energy management optimization of different FCV architectures to maximize performance. The studies focused on the use and sizing of FCREx architecture for bus applications use different EMS such as the CDCS (charge depleting and charge sustaining strategy) or two-step algorithms based on dynamic programming to analyze and optimize the vehicle costs and performance. With this, it was concluded that to minimize H_2 in FCREx the priorities are in order: reducing auxiliary power, braking energy recovery, increase FC stack efficiency, and decreasing battery losses [5]. Furthermore, following these methodologies, it was found that the optimum systems sizing design for city buses should be close to 150 Ah for the battery capacity and 40 kW for the FC system maximum power output [6]. Nonetheless, the conclusions extracted from these studies are only applicable to city buses and the performance results are far from those expected for an FCREx light passenger vehicle.

Similar to city bus application, FCREx architecture was also explored for urban logistics vehicles, using tools such as convex programming or fuzzy logic controllers to solve the sizing problem. The combination of FC systems together with moderate-capacity batteries showed that the range of urban logistics vehicles could be extended with respect to BEV and the H_2 consumption decreased by half [7]. Differently from the city bus application, the optimum battery capacity was estimated to be around 29 kWh, while the optimum FC stack maximum power depended on H_2 price [8]. The dependence of FC sizing with H_2 cost to minimize the TCO showed how sensitive the performance of FCREx vehicles is to FC stack sizing since higher FC stack maximum power implies lower H_2 consumption due to the higher system efficiency.

Among the heavy-duty applications, the use of FC for trucks is considered to provide the most advantages with respect to BEV and ICEV trucks due to the high range and carbon-free emissions. FCREx architecture is very compatible with these heavy-duty vehicles since it enables flexible operation and lower consumption. Recent research showed that using FCREx architectures for trucks could reduce the TCO by 1.3% with respect to conventional FCV architectures [9], but the result is still dependent on H_2 costs. Furthermore, different EMS were explored and compared for FCREx trucks considering 8*CHTC-HT and 7*C-WTVC Chinese truck driving cycles, concluding that convex-optimization-based EMS could provide minimal H_2 consumption and be used in on-line driving. FCREx architecture was also used in mining truck applications, where the decrease in emissions is critical to ensure the safety of mining operations, given the small space and the potential gases build-up. For these vehicles, with an optimized FC-battery hybrid powertrain design the battery life was extended, the H_2 consumption reduced, and the mining cost decreased by 8.7% [10].

Complementary to the FCREx-focused research lines, there have also been several studies also focused on EMS optimization using driving cycles simulations or conventional FCV systems sizing to improve fuel economy and system durability, but they used other components such as supercapacitors [11] or low-capacity batteries [12].

In light of the studies presented that represent the state-of-the-art of FCREx, it is worth noting that most of the use low-order models to express the FC system performance such as simple and constant polarization curves [10, 11], simple polynomials [8, 13] or simply straight lines expressing constant FC efficiency [12] that do not capture the physics behind the FC performance variation with operating conditions. In most of these studies, the FC system management was not optimized nor validated, while most of the research was focused on EMS optimization. This implies that the results were only partially-optimized and could be further improved.

The overview of the state-of-the-art research shows that currently, FCREx architecture has mostly been considered for heavy-duty applications and captive fleets such as urban logistics vehicles. Sizing studies for this architecture and applications already exist, but the conclusions and optimal designs do not apply to passenger vehicles. Furthermore, sizing studies focused on the use of FC for passenger applications do not consider FCREx architecture.

In conclusion, the literature regarding the sizing of FCREx is still limited, particularly for light passenger vehicles, and mostly omit the fundamental behavior and optimization of the FC system.

1.1. Knowledge gaps and contributions

From the analysis of the state-of-the-art, some conclusions can be extracted to provide an idea of the knowledge gaps in the literature:

1. FCREx architecture has been explored for heavy-duty vehicles such as city buses or trucks but the literature focused on using this architecture for light-duty passenger cars is limited.
2. Most of the studies do not provide the space designs generated from their sizing analyses. The results are usually based on the optimum design based on the criteria of each particular study. Generating and showing the space designs is very important to provide an estimation of the capabilities of a system, given a wide range of design combinations.
3. Range is usually not estimated for the different designs produced in the sizing analyses. In the case of FCV and FCREx, there is an actual need to understand and quantify how the sizing of the components affects the range and consumption. By showing the range estimation in design spaces, it is possible to provide passenger car manufacturers an estimation of the preliminary design they should aim for with a chosen range.
4. Most of the studies consider the FC system maximum net output power, the battery capacity, or the H_2 mass in the deposit, but very few consider these three parameters simultaneously as sizing parameters and, in the case they do, the target vehicle is a city bus instead of a light-duty passenger car.
5. The studies usually used FC system models that are not validated or, in the cases where they were validated or obtained experimentally, have not been optimized previously. Frequently, the optimization of each design was performed by optimizing only the EMS, which has a significant impact on consumption and costs reduction but does not focus on prior-optimizing the FC system behavior. Therefore, the sizing analyses usually omit the fundamental behavior and optimization of the FC system.
6. Sizing and EMS optimization are strongly coupled to provide a representative benchmarking of different designs. Some studies use the same EMS for different designs even though the load demand and the system efficiencies also change with load.
7. The resulting optimum designs from the sizing studies were not compared against commercial FCV to prove the increase in fuel economy or overall performance.

The motivation and contribution of this paper provide an understanding of the performance and costs of vehicles with FCREx architecture depending on the systems sizing and to identify how the battery capacity, the FC stack maximum power, and the H_2 tank capacity should be dimensioned depending on the target range and/or consumption. To fulfill these objectives, space designs for light-duty passenger FCREx were generated and analyzed considering as sizing variables the FC stack maximum power, the battery capacity, and the H_2 tank capacity (knowledge gaps 1, 2, 3 & 4). Unlike other studies, the FC stack model was validated at different operating conditions, the BoP operation was optimized, and the EMS between the FC stack and the battery was optimized independently for each design with the PMP (knowledge gaps 5 & 6). This means that the optimization of the FCREx was performed comprising the FC system operation and the EMS. The resulting FC system model was fully-scalable. The design spaces showing the range, the estimated systems cost, and the H_2 consumption were generated considering the WLTP driving cycle WLTC class 3b since the power-to-mass ratio of most of the designs was over 34 (this WLTC driving cycle was also chosen so that the final results can be compared against current commercial FCVs). Finally, state-of-the-art commercial FCVs were compared against equivalent-in-range optimum FCREx designs to understand the capabilities of this FCV architecture (knowledge gap 7).

1.2. Document outline

This study comprises the following parts: introduction (section 1), theoretical foundations (section 2), methodology (section 3), BoP operating conditions optimization (section 4), FCREx systems sizing (section 5), and conclusions (section 6). In the Introduction and the theoretical foundations sections, the objectives, background, and motivation of the study are defined and explained. The simulation tools and procedures were described in the methodology section. The results are presented and discussed in BoP operating conditions optimization and FCREx systems sizing sections, where the optimum operating conditions and energy balance of the FC system and the consequences of varying the FCREx design are analyzed respectively. Finally, the main conclusions of this study were summarized in the conclusions section.

2. Theoretical Foundations

2.1. H_2 as energy carrier

Hydrogen can offer numerous benefits if used as an energy carrier in most sectors. The main advantages of this fuel are its carbon-free emissions when burned or used in an FC, the possibility of producing it through different production strategies such as electrolysis or steam methane reforming (SMR), and its higher energy density in terms of mass and volume than batteries[1, 14, 15]. However, there is not such a thing as the perfect fuel, therefore H_2 has also some disadvantages if compared against batteries or conventional fuels.

Regarding the energy production sector, H_2 can be used effectively to decarbonize the gas grid. Biogas is expected not to be available at the required scale and full electrification with heat pumps would be very expensive for old buildings and would produce such seasonal imbalances in power demand that a large-scale power storage mechanism, such as H_2, would be required. Using H_2 as an energy carrier could maximize the efficiency of energy usage in the electric grid by absorbing the seasonal energy imbalances. Furthermore, its gas properties and storage versatility enable low-cost long-range renewable energy transportation through pipelines, ships, or trucks, compared to power transmission lines. The transport of H_2 could be even further optimized to reduce transportation costs and CO_2 emissions if it is first converted to any liquid e-fuel such as methanol or ethanol through CO_2 sequestration. These fuels, if produced from H_2, can also be used directly in ICE producing neutral CO_2 emissions [16, 17, 18].

In the transportation sector, H_2 has higher energy density than batteries, thus enabling long-range displacements (>500 km), and lower cradle-to-grave emissions than hydrocarbon-fueled vehicles [19], given the large variety of H_2 production strategies. Furthermore, FC systems can be easily scaled with significantly lower specific weight and power density than batteries. This makes H_2 the only option to decarbonize the operation of heavy-duty vehicles, ships, trains, and aircraft while it is a perfect fuel to complement and coexist with batteries and/or neutral CO_2 emissions ICE for light-duty vehicles, enabling high-range, carbon-free passenger cars [1, 14].

2.2. FC vehicles: non-plug-in FCV and FCREx

Fuel cell vehicles can be classified according to many criteria such as the fuel storage method (pressurized H_2 or liquid carriers to be reformed/cracked), the power system structure (direct or indirect), or the battery size (plug-in or non-plug-in). Despite all the possible classifications, it is relevant to remark how all of them are equivalent to a serial hybrid electric vehicle. Currently, the commercial FCVs Honda Clarity, Toyota Mirai, and Hyundai Nexo have an indirect-type power architecture, H_2 stored at 700 bar of pressure, and have small batteries (non-plug-in). Regarding the power system structure and the fuel storage of these vehicles, it is understandable to choose the indirect-type power architecture to reduce the size of the fuel cell system and compressed H_2 because this technology has been reliably demonstrated (high TRL) [20]. However, despite the absence of light-duty plug-in vehicles in the market, they must not be discarded since they can offer significant benefits compared to non-plug-in vehicles. These benefits are mainly lower degradation rate, potentially higher performance, increased operational flexibility, and lower TCO and cradle-to-grave emissions.

Plug-in FCVs operate using the FC like a range extender (FCREx) because both the FC and the battery can minimize power and battery state-of-charge (SOC) fluctuations. The power fluctuations that the FC stack suffers in non-plug-in vehicles operation and frequent start and stop increase their degradation [21, 22], thus leading to a decrease in performance and increase of user costs. Analogously, in-depth battery discharge or very high SOC also lead to decreased durability and performance. Therefore, keeping battery SOC in moderate and stable levels increases its life and reduces user maintenance costs [23].

Recent technological assessments of commercial FCVs show that state-of-the-art FC systems are capable of presenting highly dynamic behavior, enough to satisfy the power requirements of aggressive driving cycles with small batteries [24]. However, highly dynamic behavior induces an additional cost in performance, apart from degradation. That is why, the stable operation of FCREx could, besides, contribute to reducing H_2 consumption.

The bigger batteries of FCREx allow for a more flexible operation, enabling purely electrical mode and hybrid mode, depending on the user requirements. This is especially important in the current situation, where the price of H_2 is far above that of electricity and there are few H_2 refueling stations across the world (figure 1). In this case, these vehicles could operate as battery electric vehicles (BEV) in cities, where 100 km of range is enough since the vehicle can be charged overnight, and use the FC to extend the range for extra-urban movements with an approximate rage of 500 km.

Finally, the TCO may be lower for an FCREx if the bat-

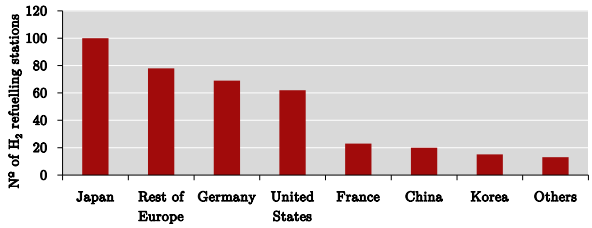

Figure 1: Hydrogen refueling stations in different countries in 2018 [14]

tery is not over-dimensioned. TCO includes the price of the vehicle, the insurance, the cost of fuel or energy source, the maintenance, and various taxes and fees. Assuming that insurance and taxes/fees are fundamentally the same for FCREx and non-plug-in FCV, FCREx could reduce the TCO due to various reasons. First, since the battery capacity is comparatively higher, the FC system maximum net power can be reduced. Hence, the stack and all the components of the FC system should have lower power requirements and should be cheaper. However, this could be outweighed by the increase in the production cost of a larger battery. Second, H_2 is currently more expensive than electricity if produced through electrolysis with the same electricity mix, therefore the operation costs of an FCV may be greater than those of a BEV. Using a mix of electricity and H_2 is an option to reduce the TCO of FCV. The option of obtaining H_2 from steam methane reforming, which should be considerably cheaper than from electrolysis, is not considered because this process produces CO_2 emissions and therefore it is not the long-term solution to sustain the vehicle portfolio of the H_2 economy [19].

3. Methodology

Studies such as optimization or sizing of vehicle systems must be carried out using simulation tools capable of representing reliably the physics of the target system. The software GT-Suite v2020 was used to perform this study. GT-Suite is a 0D-1D modeling tool widely used in the automotive industry. As such, it is capable of reproducing high fidelity numeric results based on energy, momentum, and mass conservation equations coupled with empirical correlations. 0D-1D modeling software is suitable for sizing and optimization studies since they can produce reliable results at the expense of low computational cost. However, especially for FC systems, they must be calibrated and validated with experimental data.

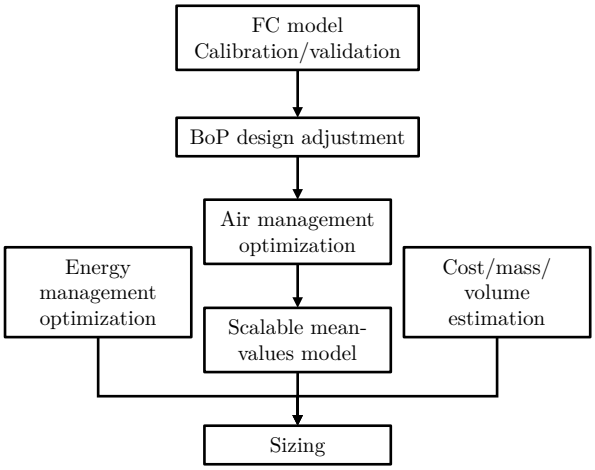

Figure 2: Methodology flow chart

As such, the first step in this study was to calibrate and validate the GT-Suite FC model using experimental data [25, 26]. Then, a model for the BoP of the FC system was adjusted to match the flow requirements of the FC stack. Next, the air management strategy of the resulting model, describing the FC system (BoP and FC stack), was optimized in steady conditions. The results from this optimization were then used to develop a mean-values model in order to reduce the computational cost of the complex model by sacrificing the FC system dynamics. For the sizing, the energy management strategy between the FC system and the battery was optimized to minimize H_2 consumption and the variation of the SoC of the battery for each design independently. GT-Suite was connected to MATLAB Simulink to perform the energy management strategy optimization. Finally, parameters such as the system costs, weight, the vehicle range, and H_2 consumption were estimated for different FCREx designs whose FC system net power, H_2 tank, and battery capacities were varied along the defined design space. This methodology is represented in figure 2.

3.1. FC model description

The polarization curve of the FC stack model used in this study is defined as follows:

$$V_{FC} = V_{OC} - V_{act} - V_{ohm} - V_{conc} \quad (1)$$

$$V_{OC} = \frac{-\Delta \bar{g}_f}{2F} \quad (2)$$

$$V_{act} = \begin{cases} \frac{R_{gas}T}{2F}\left(\frac{i}{i_0}\right) \\ \frac{R_{gas}T}{2\alpha F} ln\left(\frac{i}{i_0}\right) \end{cases} \quad (3)$$

$$V_{ohm} = R\, I \quad (4)$$

$$V_{mt} = -C\, ln\left(1 - \frac{i}{i_l}\right) \quad (5)$$

Where V_{OC} is the open voltage circuit and V_{act}, V_{ohm} and V_{mt} are the activation, ohmic and mass transport losses. Advanced losses modeling was used to include the sensitivity of the ohmic resistance and the exchange current density to the FC operating conditions. The ohmic resistance R_{ohm} was modeled according to [27] by considering the change in the ionic conductivity of the membrane as a function of the membrane water content, temperature, and membrane properties:

$$\sigma_{30} = 0.005139w - 0.00326(w > 1) \quad (6)$$

$$\sigma(T_{cell}) = exp\left[1268\left(\frac{1}{303} - \frac{1}{273 + T_{cell}}\right)\right] \quad (7)$$

$$R_{ohm} = \int^{t_m} \frac{dz}{\sigma} \quad (8)$$

Where w is the local membrane water content, σ_{30} and $\sigma(T_{cell})$ are the protonic conductivity of the membrane at 30°C and at T_{cell} respectively, T_{cell} is the cell temperature, and t_m is the membrane thickness.

Analogously, the exchange current density was modeled as a function of the FC temperature, the oxygen partial pressure, the electrochemical activation energy, the electrode roughness and the reference exchange current density $i_{0,ref}$ [28].

$$i_0 = i_{0,ref} a_c L_c \left(\frac{p_{O_2}}{p_{O_2,ref}}\right)^{\gamma_c} exp\left[\frac{-E_{act}}{RT}\left(1 - \frac{T}{T_{ref}}\right)\right] \quad (9)$$

Where $a_c L_c$ is the electrode roughness (defined by the material properties), p_{O_2} is the oxygen partial pressure, γ_c is the pressure dependency factor of the electrochemical reaction, E_{act} is the activation energy of the electrochemical reaction, R is the ideal gas constant, and T is the stack temperature.

The parameters that can be used to calibrate this formulation of the polarization curve (section 3.2) are the mass transport loss coefficient α, the exchange current density $i_{0,ref}$, the limiting current density i_l and the open circuit losses, already included into V_{OC}.

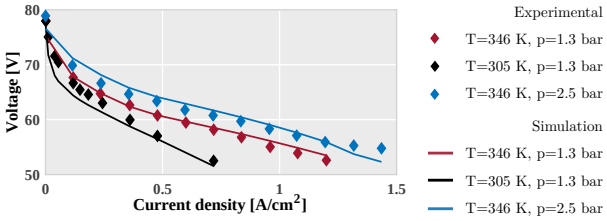

Figure 3: Calibration/validation results

Although this model was calibrated to experimental data, it still has some limitations that are not relevant for this study. For example, N_2 crossover was not modeled since the simulations of the WLTC 3b driving cycle only last 30 min (computational time), so the effect of N_2 on performance and degradation is minimum in such a short time frame. Furthermore, FC degradation was not modeled because the performance deviation due to degradation in such a short time frame is negligible. Therefore, the designs that were simulated in this study represent the maximum realistic performance of the systems. The evaluation of the degradation of the systems with the design and the EMS is out of the scope of this study.

3.2. FC model validation/calibration

The calibration of an FC stack model with experimental data is critical. Given the definition of the polarization curve, there are several coefficients and parameters that need to be calibrated (eq. 1). As such, there are several possibilities for the same polarization curve and, depending on the value of these parameters, the sensitivity of the polarization curve to boundary conditions changes. In order to validate and calibrate properly a FC stack model, it is mandatory to have data about how the polarization curve changes with temperature and pressure, i.e., the calibration should be valid for a wide range of operating conditions.

The experimental data from [25, 26] was used to calibrate the FC stack model. These data were measured from a 80 cells, 20 kW PEMFC experimental facility under temperature, stoichiometry and pressure-controlled conditions. Active surface are was assumed to be 250 cm^2. Also, the polarization curve was measured at different cathode pressure and temperature. Therefore, the data is sufficient not only to capture the polarization curve but to capture and calibrate the sensitivity to temperature and pressure of the model.

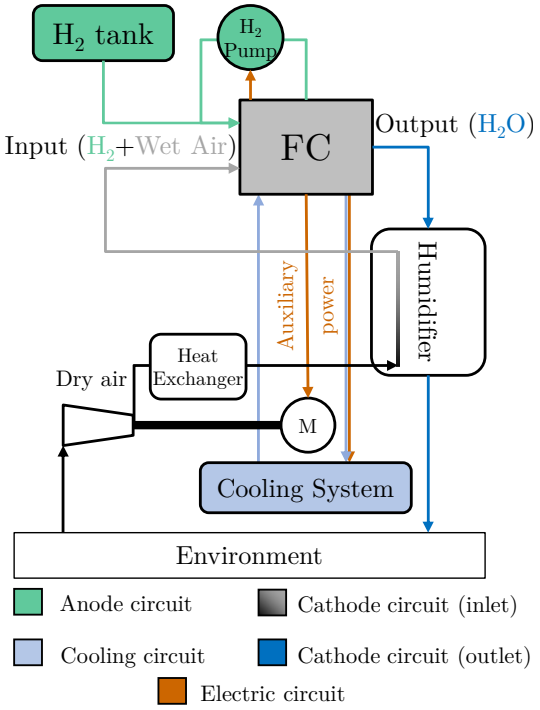

Figure 4: Fuel cell system design schematic

Genetic algorithms were used to fit the calibration parameters and coefficients describing the polarization curve simultaneously at different conditions: $T_{cath} = 346\ K$ & $p_{cath} = 1.3\ bar$, $T_{cath} = 305\ K$ & $p_{cath} = 1.3\ bar$ and $T_{cath} = 346\ K$ & $p_{cath} = 2.5\ bar$ (figure 3). Anode pressure was always kept 0.3 bar higher than cathode pressure and inlet H_2 was at ambient temperature (287 K). Stoichiometry was varied according to the experimental data [25, 26]. In order to ensure convergence of genetic algorithms, 25 generations of solutions were used. Following this methodology, it was possible to minimize the overall deviation of the model from experimental data to 2%. The higher deviations were found at low temperature at low current density. However, the error at these conditions was moderate. The sensitivity of the model to cathode stoichiometry was also validated.

3.3. FCREx vehicle architecture

3.3.1. Fuel cell system

The FC system design is composed of the FC stack and the balance of plant or BoP (figure 4). The baseline design consisted of the validated 20 kW PEMFC with its corresponding BoP. The rest of the designs in the sizing calculations were scaled versions of the baseline. The BoP architecture of all the design was maintained and

Design parameter	Value
Wheel Diameter [mm]	17.08
Compressor Speed at Design Point [rpm]	200000
Pressure ratio at Design Point [-]	1.8
Mass Flow Rate at Design Point [g/s]	9.53
Isentropic Efficiency at Design Point [%]	80

Table 1: Centrifugal compressor specifications for baseline design

can be divided into the cathode side, the anode side and the cooling side:

- The cathode side included an e-charger compressor to provide high-pressure air to the FC stack, a heat exchanger acting as an intercooler, and a humidifier system to increase the cathode inlet relative humidity (RH) using the water available in the FC stack exhaust.
  - The centrifugal compressor map was parametrized to fit the pressure and air mass flow rate requirements of the FC stack (figure 6, table 1). This was mandatory for the sizing since for different FC stack sizes the compressor specification should also change. Cathode stoichiometry and pressure were controlled through two PIDs, the first acting on the power supplied to the e-charger and the second acting on the exhaust valve area.
  - The heat exchanger was modeled with constant cooling efficiency of 70% considering the coolant at 70°C as the cold reservoir.
  - The humidifier system was modeled by 7000 pairs of 500 mm-long pipes connected by a thermal mass to include the effect of heat transfer. Water transport was modeled by means of water ejectors and injectors. The humidifier was used to keep the RH of the cathode inlet equal to 80% to ensure membrane humidification even on sudden load changes.
- The anode side included a 700 bar H_2 tank and an active H_2 recirculating loop (powered by a pump). The anode pressure was regulated by acting on the valve connecting the recirculating loop and the H_2 tank while the anode stoichiometry was controlled using the pump, powered by the FC.
- The cooling system was composed of a cooling pump, powered by the FC, and a radiator to keep the coolant temperature to 70°C. In figure 4 the

cooling system was not shown in detail for simplification purposes since it is not logistically different from those used in conventional vehicles.

The FC stack for the base configuration is that described in the previous section (20 kW PEMFC, 80 cells). Due to the lack of data provided by Corbo et al. [25, 26], the surface area and the pressure losses were modeled using the data of Ballard FCVelocity-9SSL fuel cell [29, 30]. An indirect type configuration is adapted for the vehicle, as such, a DC/DC converter is used at the output of the FC system and at the output of the battery. The DC/DC converter for the FC system is modeled considering 95% of energy conversion efficiency.
For the sizing calculations, the mass flow rate across each component was multiplied by a scaling factor, scaling also the hardware design specifications for such mass flow rates. In the case of the FC stack, the number of cells was multiplied by the scaling factor.

3.3.2. Battery

A Li-ion battery was considered for the FCREx vehicle due to the high energy density they have compared to other batteries. This battery was modeled as a set of cylindrical cells in the form of 100 serial cells to provide enough power for the purely electric mode and $n_{parallel}$ of parallel cells to impose the battery capacity. Each cylindrical cell had a nominal voltage of 3.6 V and a nominal capacity of 3.35 Ah and is modeled with an equivalent electric circuit (RC) whose open-circuit voltage and resistance depend on the state of charge and the battery temperature. A lumped mass thermal model was used to ensure that no overheating is produced in the battery. However, due to the lack of data, the effect of temperature on the battery was not accounted for. Finally, the DC/DC converter for the battery and the DC/AC converter for the electric motor were modeled with a constant conversion efficiency of 95%.

3.3.3. Vehicle body

An FCREx vehicle requires relatively high storage capacity to allocate the FC system, the H_2 tanks and the battery. As such, a vehicle body similar to that of Hyundai Nexo has been used in this study. After preliminary calculation, the vehicle has enough space to store relatively high-size batteries, given the trunk volume. The vehicle dry mass without the FC system, the H_2 tanks and the battery was estimated as 1400 kg, with a frontal area of 2.58 m^2 and a drag coefficient of 0.329, based on Hyundai Nexo technical specifications [31].

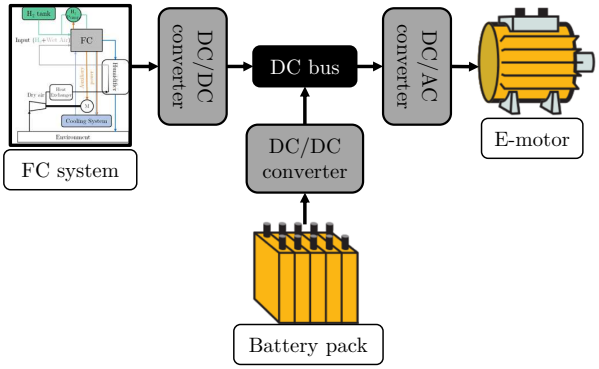

Figure 5: Powerplant electronic configuration.

The vehicle electrical architecture was decided to be indirect (figure 5). This configuration, although it could be less efficient than the direct configuration, allows to increase the FC lifetime since it is protected from the electric fluctuations of the system bus and to downsize the FC system thanks to the DC/DC converter it is connected to [20]. As mentioned before, the conversion efficiency of each DC/DC or DC/AC converters was assumed constant and equal to 95% to account for these power losses.
The device powering the shaft is an electric motor with 120 kW of maximum power whose torque-power curve provides highly-enough torque even at high load. The connection between the e-motor and the shaft was set as a direct drive.

3.4. Energy management strategy

The energy management in a powertrain with different energy sources, essentially consists of finding the sequence of power split that fulfils the design criteria with minimum cost [32]. It is a key aspect governing, to a great extent, the performance of the complete system [33]. In this sense, an inappropriate power split strategy may affect the benchmark between different sizing combinations, therefore leading to a biased decision on which is the best powertrain sizing. Optimal Control (OC) is a tool specially suited to develop the energy management strategy in a benchmark study such as the one presented in this paper, since it naturally provides the optimal energy split for every powertrain considered. Accordingly, all the architectures under investigation will be compared in the best possible scenario [34].

In line with the previous idea, the OC problem consisting of finding the powertrain control policy that minimizes a cost index over the considered driving cycle has been solved for every architecture assessed. Regarding

the control variable, considering the powertrain model described in previous sections, and particularly the energy balance in the DC bus (see figure 5, leads to:

$$P_{dem} = P_{batt} + P_{FC} \tag{10}$$

where the electrical power required by the motor to propel the vehicle (P_{dem}) can be supplied by the battery (P_{batt}), the FC (P_{FC}), or a combination of both. Note that the evolution of P_{dem} only depends on the driving cycle and therefore taking the FC power as control variable ($u = P_{FC}$)the electrical power demanded (or delivered) to the battery (P_{batt}) can be obtained as:

$$P_{batt} = P_{dem} - u \tag{11}$$

Concerning the optimization objective, the fuel consumption (H_2) has been chosen as cost to be minimized, although similarly, the fuel cost, the total energy consumed or CO_2 emissions associated to battery charging or H_2 production could be used.

Considering the chosen control variable and optimization criteria, the problem can be formally defined as finding the control law $u(t)$ over time t that minimises the cost:

$$J = \int_{t_0}^{t_f} P_f(u(t), t)\,\mathrm{dt} \tag{12}$$

where P_f is the fuel (H_2) power consumed depending on the control variable (u), in the case at hand, the electrical power delivered by the FC. Observe that as P_f is proportional to the fuel consumption, minimizing equation 12 will naturally minimize fuel consumption. The detailed FC model described in sections 3.1 and 3.3.1 was simplified to a table ($P_f = P_f(u)$) providing the fuel power P_f depending on the electrical power delivered by the FC, i.e. the control variable u.

Considering the univocal relation between u and P_f, the only state in the system is the energy stored in the battery (E_b) whose dynamic equation is:

$$\dot{E}_b = -P_b \tag{13}$$

being P_b the variation in the battery state of energy (which is considered positive when the battery is being discharged and negative when the battery is being charged). Note that P_b can be calculated from P_{batt} and the battery model described in section 3.3.2.

Finally, regarding the optimization constraints, as grid charging is not considered, and all the energy should ultimately came from the FC, the net battery charge variation in a long enough cycle should be zero to asses the battery charge sustaining and to allow a fair comparison between the powertrains considered. This is included in the optimization problem as:

$$\int_{t_0}^{t_f} P_b(u(t), E_b(t), t)\,\mathrm{dt} = 0 \tag{14}$$

Pontryagin's Minimum Principle allows solving the global optimization problem defined in equations 12-14 as a sequence of local optimization problems. In particular, the PMP states that if u^* and E_b^* are the optimal trajectories of the control and battery energy over the driving cycle, then:

$$H\left(u^*, E_b^*, \lambda^*, t\right) \leq H\left(u, E_b^*, \lambda^*, t\right) \forall u \in U, t \in [t_0, t_f] \tag{15}$$

where H is the Hamiltonian function, defined as:

$$H = P_f - \lambda \dot{E}_b = P_f(u(t), t) + \lambda(t) P_b(u(t), E_b(t), t) \tag{16}$$

Note that because P_f and P_b share the same units, the co-state λ is dimensionless. PMP identifies the evolution of λ with the variation of the Hamiltonian (H) with respect to the state (E_b):

$$\dot{\lambda} = \frac{\partial H}{\partial E_b} \tag{17}$$

Replacing equation 16 into 17 and introducing P_{batt} yields:

$$\dot{\lambda} = \lambda \frac{\partial P_b}{\partial E_b} = \lambda P_{batt} \frac{\partial (P_b / P_{batt})}{\partial E_b} \tag{18}$$

where the electrical power provided by the battery (P_{batt}), according to expression 11, depends on $u(t)$ but not on E_b. The ratio P_b/P_{batt} represents the battery efficiency. Since the sensitivity of the battery parameters (open circuit voltage and internal resistance) on variations in E_b is small, λ can be assumed constant for the considered system [35]. Therefore, the optimization problem is reduced to choose the proper constant value of λ which satisfies the problem constraint (equation 14). An extensive review of the application of PMP to the Energy Management of Hybrid Electric Vehicles can be found in [32] and references within.

As in the current work the driving cycle is known in advance, λ can be found by any iterative method, testing different values of λ until the constraint (equation 14) is satisfied. As an initial guess to the value λ, one can note that, applying the condition of minimum to equation 16 leads to:

$$\lambda = -\frac{\left(\frac{\partial P_f}{\partial u}\right)}{\left(\frac{\partial P_b}{\partial u}\right)} \tag{19}$$

Control input (u)	Fuel cell power	P_{FC}
State	Energy in the battery	E_b
Objective	Fuel minimization	eq. 12
Constraint	Charge sustaining	eq. 14
Algorithm	PMP	

Table 2: Energy management main characteristics

System	Data used to estimate Mass - Volume	Cost
FC system	Linear correlation: • Estimated 175 kg and 286 l for a 30 kW system • 250 kg and 614 l for a 70 kW system	40 \$/kW$_{net}$ ~ 36 €/kW$_{net}$
H_2 tank	0.045 kg H_2/kg system 0.030 kg H_2/l system	333 \$/kg H_2 ~ 300 €/kg H_2
Battery	220 Wh/kg 600 Wh/l	156 \$/kWh ~ 140 €/kWh

Table 3: Mass, volume and cost data [36, 37, 38, 39, 40, 41].

where terms in numerator and denominator are related to the efficiencies of FC and battery respectively, and the denominator is clearly negative due to equation 11. In this sense, the ratio between FC and battery average efficiencies is a good first guess for λ.

Table 2 summarises the details of the Energy Management Strategy

3.5. Mass, volume and cost estimation

The data to estimate the mass, volume and systems cost was obtained form different sources (table 3). Data about the systems mass had a direct impact in the simulation since it determined the vehicle total mass. In contrast, volume and cost data were only estimated for post processing purposes. Volume data was used to ensure that the H_2 tank and battery systems were small enough to fit in the rear part of the vehicle by reducing the space of the trunk. Cost estimation was performed with current data when possible or with data from DOE objectives when not public data was available. The final systems cost was used to understand which design offered the lowest production cost.

4. BoP operating conditions optimization

Prior to the sizing of the FC system, it is necessary to optimize the operating conditions of the BoP. There are several parameters affecting the performance of the FC stack such as the stoichiometry, the pressure, the temperature and the relative humidity at both the anode and the cathode. Among these parameters, the cathode stoichiometry and pressure have a major effect on

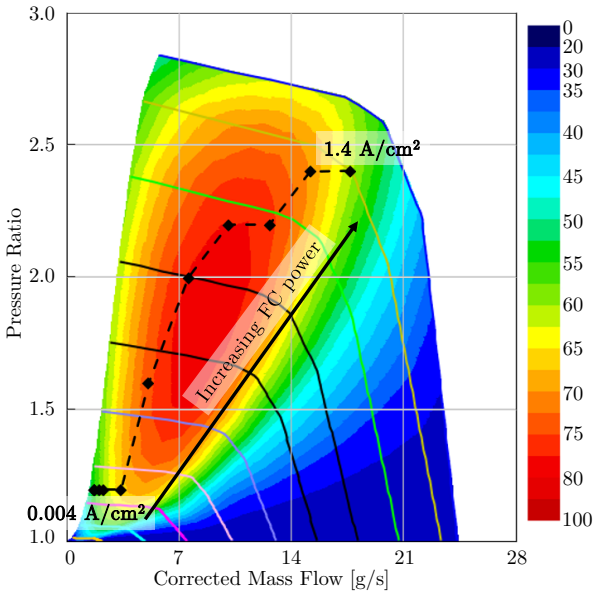

Figure 6: Parametrized compressor map with optimum operating conditions.

the FC system performance since their values are coupled with the compressor consumption, which is significantly higher than that of the H_2 recirculating pump or the coolant pump. As such, in this study, the optimization of the BoP was performed by optimizing the air management strategy with the FC stack load to maximize the FC system efficiency. The optimization was performed in steady-state conditions with some restrictions to avoid operating conditions during transient operation that may harm the integrity of the FC. As such, the cathode stoichiometry was always kept equal or over 1.8 to avoid cathode starvation during abrupt load increases, the anode pressure was always kept over the cathode pressure with a Δp limited to 0.3 bar and the minimum cathode inlet pressure was set to 1.2 bar to overcome the pressure losses of the FC stack and auxiliary devices and ensure atmospheric pressure at the outlet of the system.

Regarding the other parameters affecting the FC stack performance, some additional constraints were added:

- Anode stoichiometry was always 3 to avoid anode starvation and increase H_2 diffusion through the anode gas diffusion layer (GDL), thus maximizing the FC efficiency. This stoichiometry was kept this high because the energy consumption of the H_2 pump which controls it has a minor effect on the overall FC system.

- The relative humidity at the inlet of the cathode

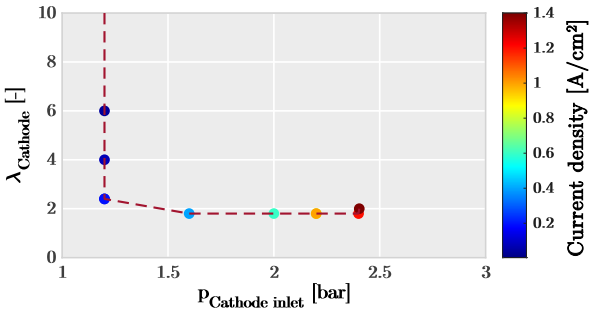

Figure 7: Optimum cathode inlet pressure and stoichiometry at different current densities (load).

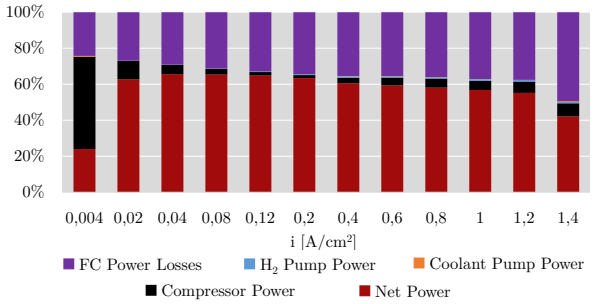

Figure 8: FC system optimum power distribution as a function of the current density.

Methodology	Design of experiments	
Control input (u)	Cathode inlet pressure	p_{cath}
	Cathode stoichiometry	λ_{cath}
Objective	Efficiency maximization	η_{FCsyst}
Constraints	Security: section 3.3.1	
	Performance: section 4	

Table 4: BoP management optimization characteristics

was 80% for any condition, i.e., the increase in temperature and pressure due to the compressor was taken into account to calculate the relative humidity.

- Coolant temperature at the outlet of the FC stack was kept to 70°C.

All these parameters were controlled by means of PID controllers as explained in section 3.3.1.

The optimization was performed for the baseline design. Since this optimization is intended to be scalable, in this section the load is expressed in terms of the current density so that it is common for all the designs (figure 7). In order to optimize the BoP operating conditions, the stoichiometry and the cathode inlet pressure were varied in the range of 1.8 to 60 (the highest values correspond to extremely low load) and from 1.2 to 2.5 bar (to preserve mechanical integrity) respectively. A summary of the main characteristics of the optimization process can be found in table 4.

From figure 6 it is possible to conclude that the optimum air management strategy of an FC system, as in ICE, is that minimizing the compressor wasted energy, i.e., for a given cathode stoichiometry (mass flow) the optimum compressor pressure ratio is that offering the maximum efficiency. This implies that the effect of increasing the FC stack fuel efficiency with air pressure has a relatively low impact on the optimization of the BoP operating conditions.

Analogously, figure 7 shows how for low loads high cathode stoichiometry was required to avoid compressor surge and the corresponding inefficiency. High pressure at high load was required only to optimize the compressor efficiency given a mass flow rate. However, as soon as the compressor can offer low stoichiometry without suffering from surge (from 0.2-0.4 A/cm^2), the cathode stoichiometry converges towards the self-imposed lower limit of 1.8, thus minimizing the compressor mass flow rate and power consumption. From this, it is possible to conclude that the driving factor when optimizing the air management strategy of an FC system is the compressor power consumption and efficiency, outweighing the increase in FC stack efficiency with cathode pressure and stoichiometry.

The optimum power distribution of the FC system is shown in figure 8. The red bar, representing the FC system net power (FC stack power minus the power consumption of the auxiliary devices), also represents the FC system efficiency. The other bars represent the power losses due to different causes such as the FC stack inefficiencies and the power consumption of the BoP (mostly compressor power consumption). As such, the curve described by joining the red bars represents the polarization curve of the FC system efficiency. In this graph it is possible to differentiate four operating regions depending on the current density:

- Ultra-low load (i $\approx$ 0.004 A/cm^2): the compressor consumes most of the power provided by the FC stack while the FC efficiency is maximum because ohmic losses are negligible. The FC system efficiency is the lowest. This region is similar to the idle condition for ICE. If available, a solution to increase the idle performance of an FC system could be to use RAM air, i.e., air directly introduced to the FC stack by bypassing the compressor to avoid the pressure loss under the low-load condition and compressed when stopped due to the relative speed

between the air and the vehicle.

- Low load (i ∈ [0.02, 0.04] A/cm^2): compared to the previous region the FC stack losses increase because ohmic losses begin to have a noticeable effect. However, FC system efficiency grows with load because the FC electrical power increases significantly compared to the compressor power.

- Medium load (i ∈ [0.04, 0.4] A/cm^2): FC system efficiency is maximized (desired operating conditions) since FC losses are moderate while the compressor power is minimized. Overall system efficiency could reach over 60%. Note that the efficiencies obtained here do not include the loss in power in the DC-DC converters and that the BoP operation was optimized and dimensioned according to the FC maximum power. This explains the slightly higher values of the efficiency in this study.

- High load (i ∈ [0.4, 1.4] A/cm^2): FC losses are almost constant up to 1.2 A/cm^2 because compressor pressure ratio increases with load. Around 1.4 A/cm^2 mass transport losses increase significantly leading to higher FC stack inefficiency. Furthermore, overall FC system efficiency decreases with load because for a given cathode stoichiometry increasing the current density means increasing the required air mass flow rate, thus increasing the compressor power consumption.

4.1. Development of the mean values model

For analyses that require a high number of simulations, the computational cost is often a limitation. In order to carry out a sizing study, it is imperative to simulate numerous designs following a *Design of Experiments* methodology. The simulation of a WLTP driving cycle considering all the FCREx systems lasts about 4 hours, making the sizing study to last about 10 months. In order to reduce the computational cost, the FC system was simplified to a mean values model, i.e., it was substituted with a map containing the steady performance and operating conditions at different loads. This model, widely used in ICE research [42, 43], interpolates linearly between previously-calculated points with relatively low error. Due to the steady nature of the model, some deviation between the complete and the mean values model was expected, especially considering the slow thermal dynamics of fuel cells affecting their transient performance.

Despite the deviation, this approach was based on a validated model under different conditions of pressure, temperature, and stoichiometry of an FC stack integrated into a BoP whose air management strategy was optimized. As such, the simplified model was capable of reproducing the actual FC system operation with simplified dynamics, providing much higher fidelity results than other approaches where the whole FC system was oversimplified to a single polarization curve without including the BoP power demand and the inefficiencies associated with driving cycle conditions. The mean values model produces lower H_2 consumption since the FC system is always working in pseudo-steady conditions, therefore the inefficiencies associated with transient operation such as slow thermal dynamics are not considered. Furthermore, the energy usage distribution in both models only presents a significant deviation in the FC system losses (figure 9) due to the error caused by model simplification. The energy usage for other purposes such as produce brake power or charge the battery with the FC stack was almost identical since the same energy management strategy was used for both models. Still, the deviation was relatively low and was accepted to reduce the computational cost from 4 hours to 50 seconds per case.

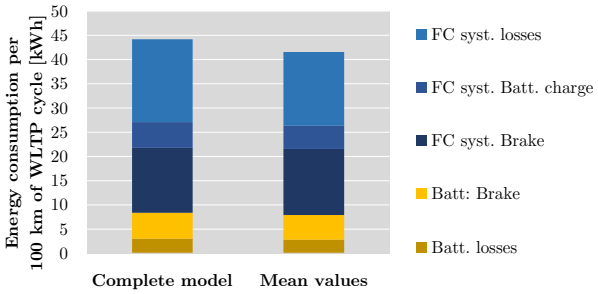

Figure 9: Energy usage distribution comparison between the complete and the mean values models.

5. FCREx systems sizing

The global space design consisted of varying 3 independent design parameters: the FC stack maximum power, the battery capacity, and the capacity of H_2 tanks. As such, the results in figures 10, 11 and 12 have 1 out of 3 parameters fixed. In the case of figure 12, the fixed parameter is the tank capacity which was set accordingly to get a specific vehicle range with an error of ±20 km. Battery capacity was varied within 30 and 60 kWh, FC stack power within 20 and 100 kW and H_2 mass in tanks within 1 and 5 kg. The ratio between the energy stored in the battery and that stored as H_2 is indicative of the H_2 usage to cover the whole range. The results provided in these figures were affected by the

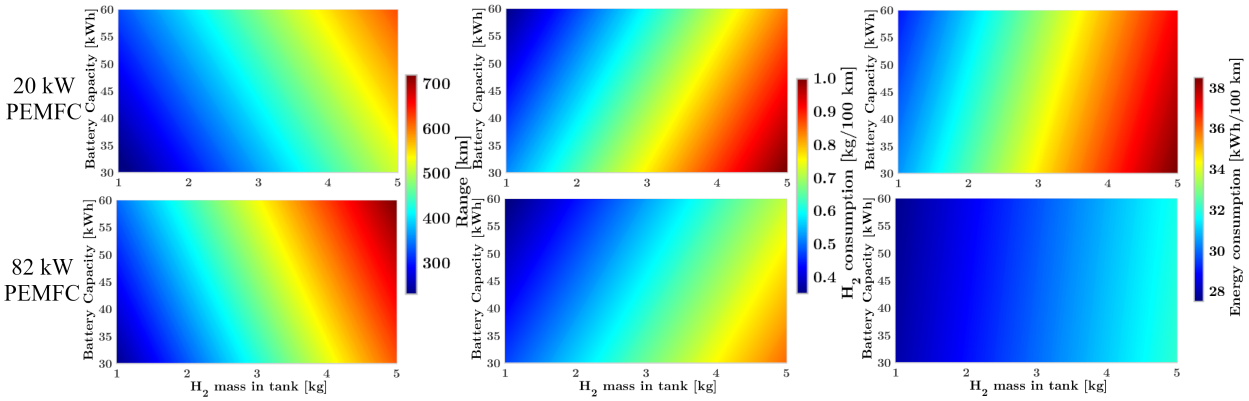

Figure 10: Range, H_2 consumption and systems cost of FCREx with 20 and 82 kW PEMFC.

error when simplifying the complete model to the mean values model. Therefore, the actual values of range may be slightly lower than those presented in figures 10 and 12.

Along this discussion, different FCREx designs are compared against state-of-the-art FCV with commercial applications. The FCV are referred as FCV1 and FCV2, and their performance data and characteristics can be found at [31] and [24], respectively.

Figure 10 shows the range, H_2 consumption and system cost as a function of the battery capacity and the H_2 tank capacity with 20 and 82 kW FC stacks. Range was calculated considering the operation with the battery until SOC=0.3, then operation with optimum energy management strategy as explained in section 3.4 until H_2 depletion, followed finally by operation until full battery discharge. In figure 10, FC stack power was the fixed design parameter in the analysis since it has the lowest influence in the range compared with the other two sized parameters. However, increasing the FC stack power implies a higher vehicle range.

When the FC stack maximum power increases, the FC system operates under lower current density for the same load. According to figure 8, this means higher FC system efficiency since the stack operates mostly in the medium current density region, i.e., lower H_2 consumption. The higher efficiency at lower current density is justified by the lower electrochemical losses and BoP power consumption. On one hand, both ohmic and activation losses decrease with the current density since the flow of protons through the membrane and the intensity of the surface reaction per unit of surface at the catalyst layer decrease, thus decreasing the losses associated with the membrane protonic conductivity (ohmic losses) and the activation overpotential required to start the electrochemical reaction (activation losses). On the other hand, since the compressor was scaled with the FC maximum power, despite the required mass flow may increase, the relative compressor energy consumption decreases since the FC stack is more efficient (see figure 8). Opposite to this effect, this also implies increasing the FC system weight, hence the vehicle weight. The increase in weight also had the effect of increasing the required load, therefore H_2 consumption. The results in the left-side and central graphs on figure 10 show that the increase in FC system efficiency outweighs the increase in the vehicle weight, thus increasing range and decreasing H_2 consumption as the FC stack maximum power increases. The left-side graphs also show how the range changes with the energy stored in the battery and the energy stored as H_2 respectively. With 20 kW PEMFC, if an iso-range line is drawn from the X axis at 2 kg of H_2 (66.6 kWh as H_2) it would cross the Y axis at about 50 kWh of energy stored in the battery. This means that from the design of 30 kWh battery and 1 kg of H_2, it would be necessary to increase the energy stored as H_2 by 33.3 kWh to get the same increase in range as increasing the battery capacity by 20 kWh. Therefore, in terms of energy utilization and performance, increasing the energy stored in the battery is more efficient to improve range than increasing it in the form of H_2 due to the higher efficiency of batteries. This additional benefit was also found with those designs whose FC maximum power was 82 kW but it was less significant since the FC efficiency increased. Despite this, the weight, space and cost restriction of batteries makes it currently impossible to achieve ranges similar to those of FCVs with BEVs for passenger vehicles. As such, to minimize energy and H_2 consumption in FCVs the battery capacity should be moderate and not reduced to the minimum as current commercial FCVs, in other words, the FCREx architecture could

also be used to maximize the energy utilization in FCVs and thus minimize consumption and maximize range.

The two central graphs of figure 10 indicate a similar decrease in H_2 consumption when the FC stack maximum power increases. As explained before, this is due to the outweigh of the FC system efficiency increase against the increase in required power when the vehicle weight increases. In this case, H_2 consumption was calculated as H_2 mass stored in the tank divided by the total range of the vehicle. Therefore, this definition is representative of the total performance of the vehicle, not only of the FC+battery mode, and is of the utmost importance given the current scenario with limited H_2 refueling stations across the globe.

As explained before, increasing the H_2 mass in the tank also increased the range. However, it also increased the H_2 consumption due to the vehicle increase in weight. This was produced because increasing the stored fuel mass did not have any effect on the efficiency of the systems directly, but increased the required power for a given operation due to the extra weight. In contrast, increasing the battery capacity dramatically decreases H_2 consumption since it implies that a greater part of the range was covered only with the battery, which implied that the range increased while the stored fuel mass was kept constant. H_2 consumption for all the designs with 82 kW PEMFC were below 0.9 kg H_2/100 km. The fuel consumption of FCV1 [31] (state-of-the-art FCV) is 0.95 kg H_2/100 km (31.6 kWh/100 km) considering 6.33 kg of H_2 stored and a range of 666 km (WLTP). Compared to this vehicle, in the design space shown in figure 10, the equivalent-in-range FCREx design with minimum H_2 consumption (4.97 kg of H_2, a battery of 44.5 kWh and 82 kW FC stack) had a H_2 consumption of 0.79 kg H_2/100 km and a total energy consumption of 31.56 kWh/100 km. Hence, this equivalent-in-range design compared to FCV1 data is capable of achieving around 16.8% saving in H_2 consumption and similar overall energy consumption to cover the whole range. This comparison allows highlighting the potential of FCREx, which could provide similar performance in terms of energy utilization and range with lower H_2 consumption and the possibility to use different driving modes depending on H_2 availability.

The right-hand side pair of graphs of figure 10 show the overall energy consumption of each design with FCREx architecture. Energy consumption was calculated as the total energy stored in the vehicle (considering both the H_2 and the battery) over the total range. Increasing the FC maximum power implied a dramatic decrease in energy consumption. This indicated that the

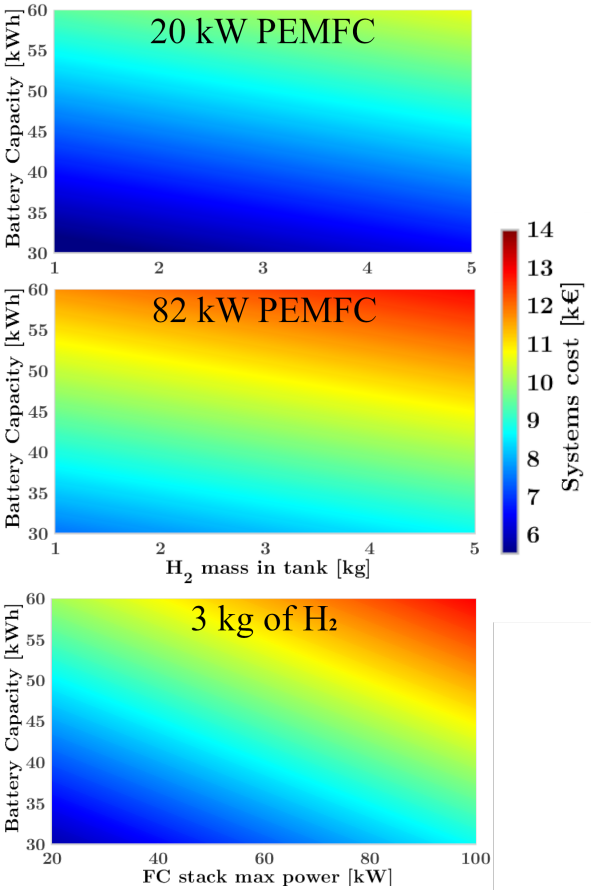

Figure 11: Total cost variation of the FC system, battery and H_2 tank for a FCREx architecture considering the designs with 20 kW PEMFC, 82 kW PEMFC and 3 kg of H_2 as fixed variables.

FC system, compared to the battery, was the most limiting system in terms of performance since it had lower efficiency. The effect of increasing the battery and the H_2 tank capacities on energy consumption was the same as that noticed on H_2 consumption. However, the effect of increasing the battery size of decreasing energy consumption was lower since for H_2 consumption the H_2 mass in the tank was kept constant. From these data, FCREx manufacturers should avoid having low-power FC stacks in their designs in order to maximize the energy utilization and range. Furthermore, FCREx also allow lower FC stack maximum power compared to FCV for the same range and performance.

The graphs in figure 11 show the total cost variation of the FC system, the battery and the H_2 tank. The two first graphs show the cost variation when extending the vehicle range by using batteries or H_2 tank capacity. Analogously, the cost variation when increasing the maximum FC stack power and the battery capacity was

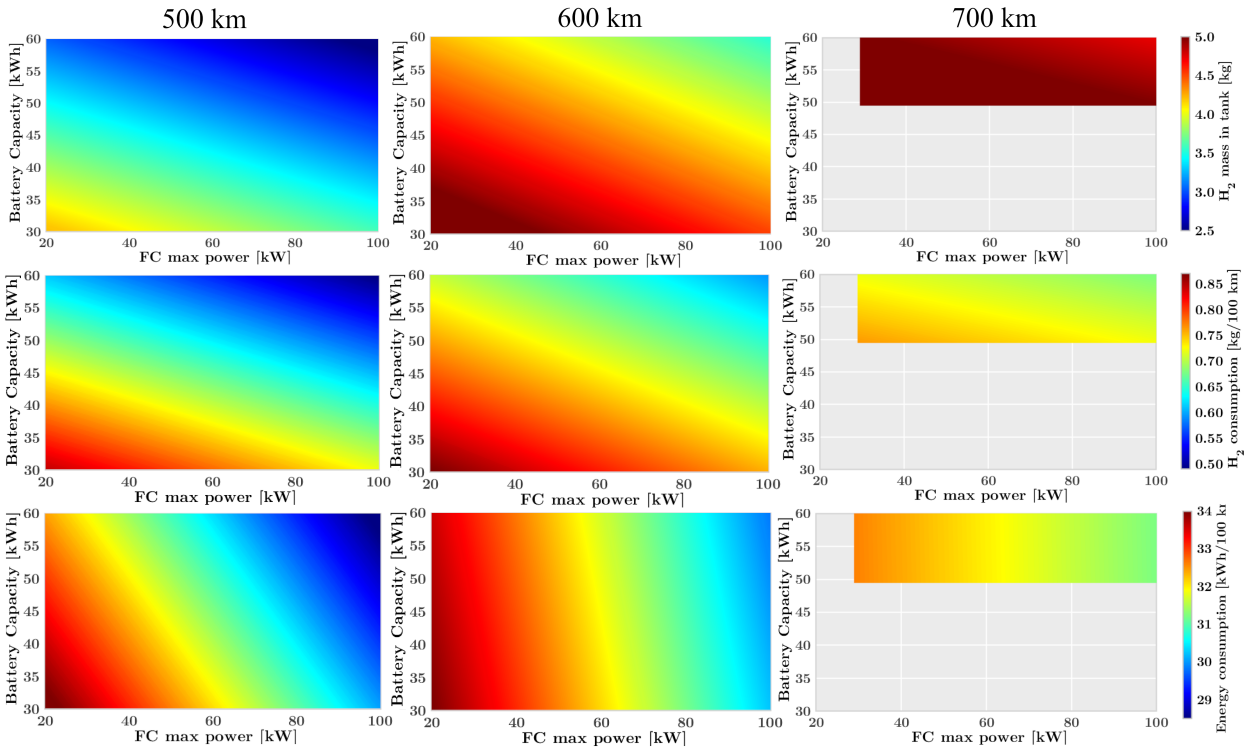

Figure 12: Design spaces showing H_2 consumption and required H_2 mass capacity for FCREx with 500, 600, 700 km of range.

showed in the third graph since these two parameters have the greatest effect on H_2 and energy consumption. From these results, increasing the energy stored in the vehicle was significantly more expensive if it was done by increasing the battery capacity rather than increasing the H_2 tank capacity. This implies that the purchase cost of any BEV with the same range as any FCV should be much higher, which could allow higher H_2 price to have the same TCO. For the designs with 82 kW PEMFC (second graph) increasing the H_2 capacity from 1 kg to 5 kg with a battery of 30 kWh was equivalent in costs to increasing the battery capacity from 30 kWh to 40 kWh with 1 kg of H_2. These two designs with equivalent cost offered significantly different performance in terms of consumption and range. The design with 5 kg of H_2 and 30 kWh of battery capacity had a range, H_2 and energy consumption of 616 km, 0.85 kg H_2/100 km and 32.1 kWh/100 km, respectively. In contrast, the design with 1 kg of H_2 and 40 kWh of battery capacity had a range, H_2 and energy consumption of 272 km, 0.43 kg H_2/100 km and 27.8 kWh/100 km, respectively. These designs are diametrically opposed and offer such different performance and range since the ratio of energy stored as H_2 to the total energy stored, including that in the battery, is completely different. This ratio was identified as another deciding factor for potential FCREx manufacturers that may change depending on the vehicle application. For the same volume of the systems, if this ratio is low (low H_2 stored), the range is significantly reduced together H_2 and energy consumption. This implies much more efficient energy usage to cover a given range, thus reducing operating costs. This architecture could be interesting for captive fleets applications such as those founds at ports and airports or for low-power vehicles, thus reducing the refueling/recharging time of these vehicles compared to BEV. In contrast, if the ratio is high, FCREx could be suitable for passenger vehicles by providing a great-enough range together with a flexible operation (battery for city driving and FC+battery for long rides) and low H_2 consumption compared to commercial FCVs. Finally, the results in figure 11 showed that increasing the FC stack maximum power also had a significant impact on the vehicle production cost. Therefore, for any car manufacturer, the final choice of the FC stack maximum power should consider the vehicle application, the increase in price and the decrease in H_2 consumption to minimize the TCO.

In figure 12, the space design for 500, 600, and 700 km of range FCREx are shown. In this case, the

mass of H_2 in the tank was fixed depending on the battery capacity to provide enough on-board energy to achieve the target range (±20 km). As such, it is possible to see that FCREx could potentially reach a range of about 700 km with 5 kg of on-board H_2, a battery of >50 kWh and a FC maximum power >30 kW if its operation was optimized. All the designs whose systems specifications were lower than these could not reach a range of 700 km due to the lack of on-board energy or the low efficiency of the systems. However, this range or slightly superior range seems to be the current limit for FCREx since the required space to have 5 kg of H_2 and a battery of >50 kWh may only be achievable for high size passenger vehicles.

Based on the results of this study, a properly designed and optimized FCREx could reach a range of 500 km with barely 3.76 kg of H_2 and a battery of 30 kWh (155.3 kWh of stored energy, i.e., 31.06 kWh/100 km of energy consumption and 0.75 kg H_2/100 km of H_2 consumption). Compared to FCV2, which has a range of approximately 500 km with 5 kg of H_2 (166.5 kWh, i.e., 33.3 kWh/100 km and 1 kg H_2/100 km of energy and H_2 consumption), this implies a much more efficient energy usage around 6.8% in energy saving and around 25% in H_2 consumption saving. As a consequence, FCREx could offer much lower operation costs.

The benefit obtained after optimizing both FCV1 and FCV2 converted into an FCREx architecture and imposing the same total range is higher in the case of the FCV2. In this case the savings in energy usage are higher (over 6% saving against no saving), and the reason is the higher fraction of the total energy stored in the battery (30 kWh out of 155.3 kWh against 44.5 kWh out of 210.15 kWh). This provides a higher optimization potential since the fraction of energy used from the battery to cover the given range increases, therefore the overall vehicle efficiency also increases accordingly.

As seen in figure 12, increasing the FC stack maximum power decreases H_2 consumption (second row of graphs in figure 12). As such, the space design shows that higher FC stack maximum power could reduce the amount of H_2 stored to reach the same range (first row of graphs in figure 12), hence reducing the operation cost but increasing the manufacturing costs. Energy consumption presents different sensitivity with the battery capacity depending on the vehicle range. For FCREx designs with 500 km of range, the decrease in energy consumption with the increase in battery capacity (due to the higher battery efficiency) is lower than for designs with 600 km of range. This happens since the ratio of stored H_2 with respect to the total on-board energy must increase to reach higher ranges, hence a higher part of the range is covered using only H_2 thus decreasing the influence of battery capacity over energy consumption. The final design of any FCREx should consider this to minimize the TCO. Based on the design spaces in figure 12 and more detailed data about the total cost of a single FCREx production, it would be possible to produce analogous graphs showing the TCO. With the data in hand, the minimum TCO would probably be located at moderate values of battery capacity (cheaper operation with only electricity from the battery) and relatively high FC stack maximum power to reduce the H_2 consumption. Of course, the optimum design to minimize the TCO depends on the H_2 price. If H_2 is cheap, the optimum would move towards lower FC stack power, lower battery capacity and higher H_2 tank capacity to reduce manufacturing costs while if it is expensive, it would move towards higher FC stack power, higher battery capacity and lower H_2 tank capacity. Estimating the TCO is a difficult task which depend on the H_2 cost, therefore on the location of the refueling station among other factors, and on the vehicle usage in general, i.e., if the vehicle is used mainly in cities (pure electric mode) and occasionally for long trips (FC+battery mode) or otherwise. This estimation is out of the scope of this study and could provide an meaningful and interesting analysis about the benefits, in terms of TCO, of FCREx against equivalent FCVs and BEVs.

As can be noticed along the discussion of results, obtaining an optimum design for FCREx passenger vehicles was not the objective of this study. Nonetheless, the generation of the design spaces enabled to understand the implications of changing the systems sizing in terms of range, production costs and consumption. Only in terms of performance, the optimum design would be that with a battery capacity of 60 kWh and a FC stack maximum power of 100 kW (figures 12), and the H_2 tank capacity would be adjusted according to the desired range. Nonetheless, this design would also imply higher manufacturing costs, compared to lower FC power designs. Following this reasoning, the optimum FCREx design would not only depend on performance factors but on the TCO, as discussed, and the cradle-to-grave emissions, which would depend significantly on the H_2 production pathway and the systems sizing. For this reason, the main outcomes of this study are the design spaces themselves together with the performance evaluation of FCREx architectures compared to current commercial FCVs, and the identification of the optimum systems sizing: moderate battery capacity (~30 kWh) and moderate-to-high FC stack maximum power (≥80 kW). Although the maximum performance was achieved for 60 kWh batteries, the increase

in systems costs almost doubled when increasing the battery capacity from 30 kWh to 60 kWh (figure 11). For that reason, the optimum design, as a trade-off between TCO and performance would most probably have a battery of 30 kWh in these design spaces. Finally, as H_2 prices drop and the FC systems become more efficient, it would be possible to reduce the FC stack maximum power output without significant variation in performance and operation costs to reduce manufacturing costs.

5.1. Results application and usefulness

The results presented in this paper can be of interest for the research community and the industry for various reasons. First, any individual from research centers or industry who wants to know which would be the optimal H_2 and/or energy consumption and range of a given FCREx design could directly use the design spaces (figures 10-12) to obtain fair and direct information. These results could be used directly in the first stages of the FCREx vehicle development process to down select an initial architecture that would be refined with costs and emissions associated data. TCO and cradle-to-grave emissions could also be obtained from H_2 and energy consumption data. Furthermore, the benefit of this architecture was highlighted against commercial FCVs, showing that the lower the total range, the higher the benefit in consumption of FCREx compared to FCV (see FCV1 and FCV2 comparisons). The maximum achievable range for a FCREx passenger with 5 kg of H_2 was also calculated (700 km), showing that FCREx architecture is suitable for passenger car application. All in all, the results presented in this study can be used extensively in both scientific research and industry applications.

6. Conclusions

In this study different space designs for FCREx vehicles were generated showing the range, the systems cost and the H_2 consumption. In order to generate such spaces a validated FC stack model was used and integrated into a FC system. The BoP operation was optimized at steady conditions. In this optimization, 3 regions of operation where identified, with the maximum FC system efficiency on the medium-load region. For these regions, the energy distribution to each component was discussed in detail. Then, the FC system model was simplified to a mean values model to reduce the computational time of a driving cycle simulation from 4 hours to 50 seconds to make the generation of the design spaces feasible. The energy management strategy was optimized for each design using the mean values model by solving the optimal control problem with the Pontryaging Minimum Principle.

The overall design space comprised the FC stack power ranging from 20 to 100 kW, the battery capacity ranging from 30 to 60 kWh and the H_2 tank capacity from 1 to 5 kg of H_2 at 700 bar. Additional design subspaces were also generated by fixing the FC maximum power to 20/82 kw or the range to 500, 600, 700 km by adjusting the battery and H_2 tank capacities to the corresponding values.

The main findings and contributions of this study are based on the understanding of the change in performance and capabilities of FCREx with the systems sizing and the identification of the benefits of FCREx architectures compared to conventional ones. Furthermore, the design spaces are a contribution themselves (figures 10-12), since they can be directly use in the first stages of FCREx design and for scientific research, as explained in section 5.1.

Regarding the performance of FCREx vehicles (figures 10 and 12), it was identified how, in general terms, increasing both the battery capacity and the FC maximum power decreases H_2 and energy consumption since the systems efficiency increase. Among these two sizing parameters, consumption is more sensitive to the FC maximum power since most of the energy stored in the FCREx vehicle was in the form of H_2. In this sense, the ratio consisting of the energy stored as H_2 over the total on-board energy in the vehicle was identified as an important parameter for potential FCREx manufacturers. For a fixed volume of the systems (available space), if this ratio is low, the range is significantly reduced together with H_2 and energy consumption (suitable for captive fleets and low-power vehicles applications). In contrast, if the ratio is high, FCREx could be suitable for passenger vehicles since they could offer great-enough range together with flexible operation (battery for city driving and FC+battery for long displacements) and lower H_2 consumption than conventional FCVs. The maximum range for FCREx could be around 700 km due to space constraints in passenger vehicles and the relation between the vehicle weight and overall efficiency.

In order to understand the benefit in performance of FCREx against conventional FCVs, equivalent-in-range FCREx designs were compared against state-of-the-art FCVs with commercial application (FCV1 & FCV2). From this comparison, it was concluded that FCREx architecture could provide a more efficient energy usage, hence lower H_2 consumption, meaning a potential decrease in the TCO. The design with a FC stack of 82 kW,

4.97 kg of H_2 and 44.5 kWh stored in the battery was equivalent in range to the FCV1 and offered 16.8% saving in H_2 consumption and similar overall energy consumption. Compared to the FCV2, the overall energy usage of the equivalent-in-range FCREx (3.76 kg of H_2 and 30 kWh of energy in the battery) was around 6.8% lower. Therefore, FCREx architecture could significantly decrease H_2 and energy consumption compared to conventional FCV.

The findings of this study, relative to the increase in performance of these vehicles with FCREx architecture, are of great relevance regarding the resources and energy utilization aspect. The combination of a high-efficiency system such as batteries together with a high specific energy system such as H_2 FC implies a clean, feasible, and efficient passenger road transport without many penalties.

In terms of systems costs (figure 11), it was concluded that increasing the range of FCREx was significantly cheaper by increasing the H_2 tank capacity rather than by increasing the battery capacity, due to the high manufacturing costs of batteries. In this sense, the total costs of the systems almost doubled when increasing the battery capacity from 30 kWh to 60 kWh. Therefore, in order to minimize manufacturing costs, it was recommended to reduce the battery capacity to the minimum to ensure enough operation with the battery mode (30 kWh).

The recommended range of optimum FCREx designs was with minimum but high-enough battery capacity (30 kWh) to reduce production costs and moderate-to-high FC maximum power (≥50 kW) to maximize performance (operation costs) since the H_2 and energy consumption was more sensitive to FC maximum power than to battery capacity. Still, an optiumu design was not selected from the design spaces since it may depend on other factors such as H_2 or electricity price (key to calculate the TCO) and cradle-to-grave emissions.

To conclude, due to the lower energy and H_2 usage than FCVs and the possibility of using electricity to cover part of the range, FCREx is a promising vehicle architecture that could reduce the TCO and cradle-to-grave emissions compared to equivalent-in-range FCVs and BEVs.

Acknowledgments

This research has been partially funded by FEDER and the Spanish Government through project RTI2018-102025-B-I00 (CLEAN-FUEL) and through the University Faculty Training (FPU) program.

References

[1] Fuel Cells & Hydrogen (FCH), Hydrogen Roadmap Europe - a Sustainable Pathway for the European Energy Transition, 1st Edition, Publications Office of the European Union, 2019. doi:10.2843/341510.

[2] B. Lane, B. Shaffer, S. Samuelsen, A comparison of alternative vehicle fueling infrastructure scenarios, Applied Energy 259 (June 2019) (2020) 114128. doi:10.1016/j.apenergy.2019.114128.

[3] D. Feroldi, M. Carignano, Sizing for fuel cell/supercapacitor hybrid vehicles based on stochastic driving cycles, Applied Energy 183 (2016) 645–658. doi:10.1016/j.apenergy.2016.09.008.

[4] M. Pourabdollah, B. Egardt, N. Murgovski, A. Grauers, Convex optimization methods for powertrain sizing of electrified vehicles by using different levels of modeling details, IEEE Transactions on Vehicular Technology 67 (3) (2018) 1881–1893.

[5] L. Xu, M. Ouyang, J. Li, F. Yang, L. Lu, J. Hua, Optimal sizing of plug-in fuel cell electric vehicles using models of vehicle performance and system cost, Applied Energy 103 (2013) 477–487. doi:10.1016/j.apenergy.2012.10.010.

[6] L. Xu, C. D. Mueller, J. Li, M. Ouyang, Z. Hu, Multi-objective component sizing based on optimal energy management strategy of fuel cell electric vehicles, Applied Energy 157 (2015) 664–674. doi:10.1016/j.apenergy.2015.02.017.

[7] X. Lü, P. Wang, L. Meng, C. Chen, Energy optimization of logistics transport vehicle driven by fuel cell hybrid power system, Energy Conversion and Management 199 (June) (2019) 111887. doi:10.1016/j.enconman.2019.111887.

[8] X. Wu, X. Hu, X. Yin, L. Li, Z. Zeng, V. Pickert, Convex programming energy management and components sizing of a plug-in fuel cell urban logistics vehicle, Journal of Power Sources 423 (March) (2019) 358–366. doi:10.1016/j.jpowsour.2019.03.044.

[9] K. Sim, R. Vijayagopal, N. Kim, A. Rousseau, Optimization of component sizing for a fuel cell-powered truck to minimize ownership cost, Energies 12 (6) (2019). doi:10.3390/en12061125.

[10] Y. Feng, Z. Dong, Integrated design and control optimization of fuel cell hybrid mining truck with minimized life-cycle cost, Applied Energy 270 (March) (2020) 115164. doi:10.1016/j.apenergy.2020.115164.

[11] S. D. Gaikwad, P. C. Ghosh, Sizing of a fuel cell electric vehicle: A pinch analysis-based approach, International Journal of Hydrogen Energy 45 (15) (2020) 8985–8993. doi:10.1016/j.ijhydene.2020.01.116.

[12] Z. Hu, J. Li, L. Xu, Z. Song, C. Fang, M. Ouyang, G. Dou, G. Kou, Multi-objective energy management optimization and parameter sizing for proton exchange membrane hybrid fuel cell vehicles, Energy Conversion and Management 129 (2016) 108–121. doi:10.1016/j.enconman.2016.09.082.

[13] X. Wu, X. Hu, X. Yin, Y. Peng, V. Pickert, Convex programming improved online power management in a range extended fuel cell electric truck, Journal of Power Sources 476 (2019) (2020) 228642. doi:10.1016/j.jpowsour.2020.228642.

[14] International Energy Agency, The Future of Hydrogen, Tech. Rep. June (2019). doi:10.1787/1e0514c4-en.

[15] S. Verhelst, T. Wallner, Hydrogen-fueled internal combustion engines, Progress in Energy and Combustion Science 35 (6) (2009) 490–527. doi:10.1016/j.pecs.2009.08.001.

[16] J. Benajes, G. Antonio, J. Monsalve-Serrano, I. Balloul, G. Pradel, Evaluating the reactivity controlled compression ignition operating range limits in a high-compression ratio medium-duty diesel engine fueled with biodiesel and ethanol,

International Journal of Engine Research 18 (2017) 60–88. doi:10.1177/1468087416678500.
[17] A. García, J. Monsalve-Serrano, D. Villalta, R. Lago Sari, V. Gordillo Zavaleta, P. Gaillard, Potential of e-Fischer Tropsch diesel and oxymethyl-ether (OMEx) as fuels for the dual-mode dual-fuel concept, Applied Energy 253 (2019) 113622. doi:10.1016/j.apenergy.2019.113622.
[18] A. García, J. Monsalve-Serrano, E. José Sanchís, Á. Fogué-Robles, Exploration of suitable injector configuration for dual-mode dual-fuel engine with diesel and OMEx as high reactivity fuels, Fuel 280 (2020) 118670. doi:10.1016/j.fuel.2020.118670.
[19] J. M. Desantes, S. Molina, R. Novella, M. Lopez-Juarez, Comparative global warming impact and NOX emissions of conventional and hydrogen automotive propulsion systems, Energy Conversion and Management 221 (2020) 113137. doi:10.1016/j.enconman.2020.113137.
[20] T. Teng, X. Zhang, H. Dong, Q. Xue, A comprehensive review of energy management optimization strategies for fuel cell passenger vehicle, International Journal of Hydrogen Energy 45 (39) (2020). doi:10.1016/j.ijhydene.2019.12.202.
[21] Z. Sun, Y. Wang, Z. Chen, X. Li, Min-max game based energy management strategy for fuel cell/supercapacitor hybrid electric vehicles, Applied Energy 267 (2020) 115086. doi:10.1016/j.apenergy.2020.115086.
[22] H. Zhang, X. Li, X. Liu, J. Yan, Enhancing fuel cell durability for fuel cell plug-in hybrid electric vehicles through strategic power management, Applied Energy 241 (January) (2019) 483–490. doi:10.1016/j.apenergy.2019.02.040.
[23] E. Wikner, T. Thiringer, Extending battery lifetime by avoiding high SOC, Applied Sciences (Switzerland) 8 (10) (2018). doi:10.3390/app8101825.
[24] Argonne National Laboratory, Technology Assessment of a Fuel Cell Vehicle: 2017 Toyota Mirai Energy Systems Division, US DOE -Energy Systems Division (2017).
[25] P. Corbo, F. Migliardini, O. Veneri, Experimental analysis and management issues of a hydrogen fuel cell system for stationary and mobile application, Energy Conversion and Management 48 (8) (2007) 2365–2374. doi:10.1016/j.enconman.2007.03.009.
[26] P. Corbo, F. Migliardini, O. Veneri, Experimental analysis of a 20 kWe PEM fuel cell system in dynamic conditions representative of automotive applications, Energy Conversion and Management 49 (10) (2008) 2688–2697. doi:10.1016/j.enconman.2008.04.001.
[27] I. Terada, H. Nakagawa, Polymer Electrolyte Fuel Cell, Kobunshi 57 (7) (2008) 498–501. doi:10.1295/kobunshi.57.498.
[28] D. Murschenhofer, D. Kuzdas, S. Braun, S. Jakubek, A real-time capable quasi-2D proton exchange membrane fuel cell model, Energy Conversion and Management 162 (January) (2018) 159–175. doi:10.1016/j.enconman.2018.02.028.
[29] Ballard, FCvelocity – 9SSL product specification (2011).
[30] R. A. Rabbani, Dynamic Performance of a PEM Fuel Cell System, DTU Mechanical Engineering. DCAMM Special Report (No. S154) (2013).
[31] Hyundai, Hyundai Nexo - Technical Specifications.
[32] S. Onori, L. Serrao, G. Rizzoni, Hybrid electric vehicles: Energy management strategies, Springer, 2016.
[33] A. Sciarretta, L. Guzzella, Control of hybrid electric vehicles, IEEE Control Systems Magazine 27 (2) (2007) 60–70.
[34] J. M. Luján, C. Guardiola, B. Pla, A. Reig, Cost of ownership-efficient hybrid electric vehicle powertrain sizing for multi-scenario driving cycles, Proceedings of the Institution of Mechanical Engineers, Part D: Journal of Automobile Engineering 230 (3) (2016) 382–394.
[35] L. Serrao, S. Onori, G. Rizzoni, Ecms as a realization of pontryagin's minimum principle for hev control, in: 2009 American control conference, IEEE, 2009, pp. 3964–3969.
[36] Ballard, Product Data Sheet - FCMove-HD (2016).
[37] Ballard, Product Data Sheet - FCVelocity-MD (2016).
[38] U.S. Department Of Energy, DOE Technical Targets for Fuel Cell Systems and Stacks for Transportation Applications (2015).
[39] U.S. Department Of Energy, DOE Technical Targets for Onboard Hydrogen Storage for Light-Duty Vehicles (2015).
[40] D. Howell, B. Cunningham, T. Duong, P. Faguy, Overview of the DOE VTO Advanced Battery R&D Program, Tech. rep., U.S. Department Of Energy (2016).
[41] BloombergNEF, 2019 Battery Price Survey, Tech. rep. (2019).
[42] J. M. Luján, C. Guardiola, B. Pla, A. Reig, Optimal control of a turbocharged direct injection diesel engine by direct method optimization, International Journal of Engine Research 20 (6) (2019) 640–652.
[43] F. Payri, C. Guardiola, B. Pla, D. Blanco-Rodriguez, A stochastic method for the energy management in hybrid electric vehicles, Control Engineering Practice 29 (2014) 257–265. doi:10.1016/j.conengprac.2014.01.004.